

# JGR Atmospheres

## RESEARCH ARTICLE

10.1029/2024JD041368

### Key Points:

- *n*-Alkanes and PAHs can show stronger sorption to particulate matter (PM) than in the simulation based on the equilibrium absorptive partitioning theory
- Combining absorption and adsorption mechanisms can improve the agreement between measured and predicted partitioning coefficients
- The sorption of *n*-alkanes and PAHs on PM is less liquid-like in Denver than in Nanjing

### Supporting Information:

Supporting Information may be found in the online version of this article.

### Correspondence to:

M. Xie,  
[mingjie.xie@nuist.edu.cn](mailto:mingjie.xie@nuist.edu.cn);  
[mingjie.xie@colorado.edu](mailto:mingjie.xie@colorado.edu)

### Citation:

Zhou, Z., Wang, Z., Feng, W., Qin, C., Liao, H., Wang, Y., & Xie, M. (2024). Simulation of gas-particle partitioning of semi-volatile *n*-alkanes and PAHs in Nanjing, China, and Denver, United States: Effects of vapor pressure and surface adsorption estimation. *Journal of Geophysical Research: Atmospheres*, 129, e2024JD041368. <https://doi.org/10.1029/2024JD041368>

Received 12 APR 2024


Accepted 19 SEP 2024

### Author Contributions:

**Conceptualization:** Mingjie Xie  
**Data curation:** Zishu Wang  
**Formal analysis:** Zhiyan Zhou, Wei Feng  
**Funding acquisition:** Mingjie Xie  
**Investigation:** Zhiyan Zhou, Zishu Wang  
**Methodology:** Mingjie Xie  
**Project administration:** Mingjie Xie  
**Resources:** Chao Qin, Hong Liao, Yuhang Wang  
**Supervision:** Mingjie Xie  
**Validation:** Wei Feng  
**Writing – original draft:** Zhiyan Zhou  
**Writing – review & editing:** Chao Qin, Hong Liao, Yuhang Wang, Mingjie Xie

© 2024. American Geophysical Union. All Rights Reserved.

## Simulation of Gas-Particle Partitioning of Semi-Volatile *n*-Alkanes and PAHs in Nanjing, China, and Denver, United States: Effects of Vapor Pressure and Surface Adsorption Estimation

Zhiyan Zhou<sup>1</sup>, Zishu Wang<sup>2</sup>, Wei Feng<sup>1</sup>, Chao Qin<sup>3</sup>, Hong Liao<sup>1</sup> , Yuhang Wang<sup>4</sup> , and Mingjie Xie<sup>1</sup> 

<sup>1</sup>Collaborative Innovation Center of Atmospheric Environment and Equipment Technology, Jiangsu Key Laboratory of Atmospheric Environment Monitoring and Pollution Control, School of Environmental Science and Engineering, Nanjing University of Information Science & Technology, Nanjing, China, <sup>2</sup>Nuist Reading Academy, Nanjing University of Information Science & Technology, Nanjing, China, <sup>3</sup>State Environmental Protection Key Laboratory of Monitoring and Analysis for Organic Pollutants in Surface Water, Jiangsu Environmental Monitoring Center, Nanjing, China, <sup>4</sup>School of Earth and Atmospheric Sciences, Georgia Institute of Technology, Atlanta, GA, USA

**Abstract** The concentration data of semi-volatile *n*-alkanes and PAHs in the gas phase and in PM<sub>2.5</sub> were obtained from Nanjing and Denver. First, the gas-particle partitioning coefficients of the target compounds were calculated and compared with the predictions based on the equilibrium absorptive partitioning theory. Although the vapor pressure ( $p^{\circ}_L$ ) estimation method was selected to improve the agreement between measured and predicted partitioning coefficients, *n*-alkanes in Denver and PAHs in both cities exhibited stronger sorption to PM<sub>2.5</sub> than predicted. By including the adsorption mechanism, the average logarithms and temporal variations of the partitioning coefficients were well simulated in both Nanjing and Denver. The partitioning of *n*-alkanes in Nanjing can be primarily explained by the absorption mechanism, while the adsorption mechanism dominates that for *n*-alkanes in Denver and PAHs in both cities. To obtain an optimal simulation, the  $p^{\circ}_L$  of *n*-alkanes and PAHs was estimated using the SPARC and SIMPOL—two group contribution methods, respectively, and the difference between desorption and vaporization enthalpies was set between 2 and 3 kcal mol<sup>-1</sup> for *n*-alkanes in Denver and PAHs in both cities. Therefore, the estimation of  $p^{\circ}_L$  and surface adsorption should be carefully considered when parameterizing the gas-particle partitioning of non-polar organic compounds in future field and modeling studies.

**Plain Language Summary** The gas-particle partitioning of semi-volatile organic compounds is an important atmospheric process that can affect their fate and transport. The concentrations of selected *n*-alkanes and PAHs significantly present in both the gas and particulate phases in Nanjing and Denver were obtained from our previous studies. When absorption in particulate organic matter (OM) was assumed as the dominant mechanism, the gas-particle partitioning of *n*-alkanes in Denver and PAHs in both cities cannot be well explained. When both absorption in the particulate OM phase and surface adsorption were considered, good agreement between measured and predicted partitioning coefficients could be obtained for all target compounds by selecting an appropriate method to estimate the vapor pressure ( $p^{\circ}_L$ ) and fixing the difference between desorption and vaporization enthalpies. In previous studies, the simulated partitioning coefficients differed by orders of magnitude from the measured values, partly due to the ignorance of  $p^{\circ}_L$  estimation method selection and surface adsorption.

## 1. Introduction

Semi-volatile organic compounds (SVOCs) have a wide range of vapor pressures ( $10^{-14}$  to  $10^{-4}$  atm; Weschler & Nazaroff, 2008). The partitioning between the gas and condensed phases of SVOCs plays an important role in influencing their fate and transport in the atmosphere (Bidleman, 1988; Liang et al., 1997) and is also a pivotal process for the formation of secondary organic aerosols (SOA) through photochemical reactions and reactive uptake of gaseous oxygenated intermediates (Donahue et al., 2006; Hallquist et al., 2009). Early studies parameterized the gas-particle partitioning of SVOCs based on the concentrations of particulate matter (PM) and individual organic compounds in ambient air (Pankow & Bidleman, 1992; Yamasaki et al., 1982):

$$K_p = \frac{F/TSP}{A} \quad (1)$$

where  $K_p$  ( $\text{m}^3 \mu\text{g}^{-1}$ ) is the partitioning coefficient, TSP ( $\mu\text{g m}^{-3}$ ) is the mass concentration of the total suspended PM, and  $F$  ( $\text{ng m}^3$ ) and  $A$  ( $\text{ng m}^3$ ) are the particle and gas phase concentrations of the target compounds, respectively. Pankow (1994a, 1994b) developed a partitioning model to predict the contributions of absorption and adsorption mechanisms to  $K_p$ :

$$K_p = \frac{1}{p_L^0} \left[ N_s a_{\text{TSP}} R T e^{(Q_1 - Q_v)/RT} + \frac{f_{\text{OM}} R T}{10^6 \text{MW}_{\text{OM}} \zeta_{\text{OM}}} \right] \quad (2)$$

where the first term in the brackets depicts the physical adsorption on the particle surfaces, and the second term represents equilibrium absorptive partitioning towards the organic matter (OM) phase in PM. In the adsorption term,  $N_s$  ( $\text{mol cm}^{-2}$ ) is the surface concentration of adsorption sites,  $a_{\text{TSP}}$  ( $\text{m}^2 \text{g}^{-1}$ ) is the specific surface area of total suspended PM,  $R$  is the gas constant (e.g.,  $8.21 \times 10^{-5} \text{m}^3 \text{atm mol}^{-1} \text{K}^{-1}$ ),  $T$  is the temperature (K),  $Q_1$  and  $Q_v$  ( $\text{kJ mol}^{-1}$ ) are the enthalpies of desorption and vaporization, respectively. For the absorption mechanism,  $f_{\text{OM}}$  is the mass fraction (%) of the OM phase in the total PM,  $\text{MW}_{\text{OM}}$  ( $\text{g mol}^{-1}$ ) is the mean molecular weight (MW) of the OM phase,  $\zeta_{\text{OM}}$  is the activity coefficient of a given compound in the OM phase on the mole fraction scale. In Equation 2,  $p_L^0$  (atm) is the vapor pressure of each pure compound at the temperatures during sampling. The equilibrium absorptive partitioning has been proposed as the dominant mechanism (Liang et al., 1997; Liang & Pankow, 1996; Mader & Pankow, 2002) and applied to predict the SOA yield in the smoke chamber and the ambient (Beardsley & Jang, 2016; Odum et al., 1996; Zhang et al., 2022). The measured and predicted partitioning coefficients based on the equilibrium absorption mechanism can be calculated as follows

$$K_{\text{p,OM}}^{\text{m}} = \frac{K_p}{f_{\text{OM}}} = \frac{F/M_{\text{OM}}}{A} \quad (3)$$

$$K_{\text{p,OM}}^{\text{t}} = \frac{RT}{10^6 \text{MW}_{\text{OM}} \zeta_{\text{OM}} p_L^0} \quad (4)$$

where  $K_{\text{p,OM}}^{\text{m}}$  and  $K_{\text{p,OM}}^{\text{t}}$  are measured and predicted absorptive partitioning coefficients ( $\text{m}^3 \mu\text{g}^{-1}$ ), and  $M_{\text{OM}}$  ( $\mu\text{g m}^{-3}$ ) is the concentration of the OM phase in PM.

The reactions of secondary organics in the condensed phase and their absorptive partitioning to aerosol liquid water (ALW) are potential reasons for the underestimation of SOA production by assuming that particulate OM is the only absorbing phase under ideal mixing conditions (Barsanti et al., 2013; Daumit et al., 2016; Healy et al., 2008; Kampf et al., 2013; Pye et al., 2017; Yu et al., 2021). In contrast, the base-10 logarithms of  $K_{\text{p,OM}}^{\text{m}}$  ( $\lg K_{\text{p,OM}}^{\text{m}}$ ) and  $p_L^0$  ( $\lg p_L^0$ ) of non-polar SVOCs (e.g., PAHs) are strongly correlated with regression slopes fluctuating around  $-1.0$  (Gou et al., 2021; Liang et al., 1997), suggesting that their gas-particle partitioning is a temperature-controlled process associated with the OM phase in PM. Therefore, the agreement between  $K_{\text{p,OM}}^{\text{m}}$  and  $K_{\text{p,OM}}^{\text{t}}$  for each SVOC may strongly depend on the reasonableness of  $p_L^0$  estimation. In addition, the effect of adsorption on particle surfaces cannot be excluded under certain circumstances. For example, polycyclic aromatic compounds (PAHs) exhibit stronger sorption than  $n$ -alkanes at a given  $p_L^0$  possibly due to the  $\pi$ - $\pi$  interactions between PAHs and PM surfaces (Cousins & Mackay, 2001; Liang & Pankow, 1996; Zhu et al., 2004). Except for the influences of  $p_L^0$  estimation and surface adsorption, the discrepancies between  $K_{\text{p,OM}}^{\text{m}}$  and  $K_{\text{p,OM}}^{\text{t}}$  observed in previous studies could also be caused by measurement artifacts, variations in  $\text{MW}_{\text{OM}}$  and  $\zeta_{\text{OM}}$ , non-ideal mixing, etc (Cappa et al., 2008; Chang & Pankow, 2010; Pankow & Bidleman, 1992; Pankow & Chang, 2008; Wang et al., 2015).

In this work, measurement data of selected  $n$ -alkanes and PAHs in the gas phase and in  $\text{PM}_{2.5}$  were obtained from Nanjing, China, and Denver, United States. The measured and predicted partitioning coefficients of these SVOCs were calculated based on Equations 1–4. For the prediction of partitioning coefficients, the  $p_L^0$  values of individual compounds were estimated by three methods, and three  $Q_1$ – $Q_v$  values were considered for the evaluation of

the adsorption mechanism. The study results will improve our understanding and simulation of the gas-particle partitioning of non-polar SVOCs in the atmosphere.

## 2. Methods

### 2.1. Measurement Data Preparation

The measurement data for *n*-alkanes and PAHs in the cities of Nanjing and Denver were obtained from Gou et al. (2021) and Xie et al. (2014). In these two studies, gaseous and particulate SVOCs were measured using a similar method. In brief, ambient air was drawn through two stacked pre-baked quartz filters and a sandwich cartridge of polyurethane foam (PUF)/XAD-4 resin/PUF (PXP) by a medium-volume sampler equipped with a 2.5 μm cut impactor or cyclone. Non-polar SVOCs in filter and PXP samples were extracted with dichloromethane and analyzed with an Agilent 7890B gas chromatograph (GC) coupled to an Agilent 5977B mass spectrometer (MS). Total organic carbon (OC) and elemental carbon (EC) on the filter samples were measured using a thermal optical ECOC analyzer. The upper filter ( $Q_f$ ) was used to determine the  $PM_{2.5}$  mass through gravimetric analysis and particle-phase organics. SVOCs on the backup filter ( $Q_b$ ) were assumed to be contributed equally by gaseous adsorption (“blow on,” positive artifact) and evaporative losses from  $Q_f$  (“blow off,” negative artifact). The PXP cartridge was installed for the adsorption of gaseous SVOCs. Therefore, in this work, the particle phase concentrations of the target compounds were defined as their concentrations in  $Q_f$  samples, and the total concentrations of the target compounds in  $Q_b$  and PXP samples were treated as their gas phase concentrations.

The organic compounds with extremely high ( $>10^{-6}$  atm) or low  $p_L^o$  ( $<10^{-10}$  atm) exist almost exclusively in one phase (gas or particle phase), and their concentrations in the other phase can be very low and subject to great uncertainty. Therefore, the *n*-alkanes and PAHs selected for analysis in this work have significant concentrations in both the gas and particle phases. Information on the selected *n*-alkanes (6 species, carbon number = 18–23) and PAHs (5 species, MW = 178–228) is provided in Table 1. A total of 102 pairs of 12-hr gas-phase and particle-phase samples of the above compounds were obtained at a suburban site in northern Nanjing from 28 September 2018 to 29 September 2019 (Gou et al., 2021); 50 pairs of 24-hr samples of the same species were obtained at an urban site in Denver from 28 August 2012 to 25 July 2013 (Xie et al., 2014). The average concentrations of *n*-alkanes and PAHs in the gas and particulate phases and their average particle-phase fractions ( $F\%$ ) in Nanjing and Denver are summarized in Table 2. As the target compounds were not detected in the particle and/or gas phase for some sample pairs, especially for low volatile species (e.g., *n*-C23, BaA, and CT) in the gas phase during the cold period, these observations were not included in the calculation of  $F\%$  and partitioning coefficients.

### 2.2. Calculations of the Partitioning Coefficients

The  $K_{p,OM}^m$  values of the target compounds were calculated using Equation 3, where  $M_{OM}$  was defined as the concentration of OC in  $PM_{2.5}$  multiplied by 1.6 (Turpin & Lim, 2001), and their  $K_{p,OM}^t$  values were calculated using Equation 4. For each sample, the  $p_L^o$  values of the target compounds were adjusted based on the average temperature:

$$p_L^o = p_L^{o,*} \exp \left[ \frac{Q_v^*}{R} \left( \frac{1}{298.15} - \frac{1}{T} \right) \right] \quad (5)$$

where  $p_L^{o,*}$  and  $Q_v^*$  are the subcooled liquid vapor pressure (atm) and the enthalpy of vaporization ( $\text{kJ mol}^{-1}$ ) at 298.15 K. To evaluate the impact of  $p_L^o$  estimation on the agreement between  $K_{p,OM}^m$  and  $K_{p,OM}^t$ ,  $p_L^{o,*}$  was predicted using three methods, including the U.S. Environmental Protection Agency's Toxicity Estimation Software Tool (TEST; EPA, 2022) and the group contribution methods (GCMs) SPARC (<http://archemcalc.com/sparc-web/calc/>) and SIMPOL (Pankow & Asher, 2008; Table 1). Literature  $p_L^{o,*}$  values from indirect measurements based on the temperature dependence of GC retention times are also listed in Table 1. Xie et al. (2013) have tested the sensitivity of  $K_{p,OM}^t$  to changes in temperature (276.5–297.6 K),  $MW_{OM}$  (50–300  $\text{g mol}^{-1}$ ),  $\zeta_{OM}$  (0.5–1.5), and OM/OC ratios (1.3–1.6). Since  $p_L^o$  increased exponentially with temperature (Equation 5) and varied by more than an order of magnitude within 20 K,  $K_{p,OM}^t$  is most sensitive to ambient temperature. Due to the large variability in ambient temperature during sampling (Table 2) and  $p_L^{o,*}$  values across the three estimation methods (Table 1), the selection of  $p_L^{o,*}$  estimation method was prioritized in the prediction of  $K_{p,OM}^t$ , and the

**Table 1**

Predicted Liquid-State Vapor Pressure ( $p^{o,*}_L$ , Atm) and Vaporization Enthalpy ( $Q^*_v$ , kJ Mol<sup>-1</sup>) of Selected *n*-Alkanes and PAHs at 298.15 K

Species	Abbr.	MW	$p^{o,*}_L$				$Q^*_v$			
			TEST <sup>a</sup>	SPARC <sup>b</sup>	SIMPOL <sup>b</sup>	Measurement-based estimation	TEST <sup>a</sup>	SPARC <sup>b</sup>	SIMPOL <sup>b</sup>	Measurement-based estimation
<i>n</i> -Alkanes										
octadecane	<i>n</i> -C18	254	$1.83 \times 10^{-7}$	$1.58 \times 10^{-7}$	$5.81 \times 10^{-7}$	$1.98 \times 10^{-7,c}$	85.2	89.3	99.2	91.4 <sup>c</sup>
nonadecane	<i>n</i> -C19	268	$1.15 \times 10^{-7}$	$5.5 \times 10^{-8}$	$2.01 \times 10^{-7}$	$6.37 \times 10^{-8,c}$	87.0	94.3	104	96.4 <sup>c</sup>
eicosane	<i>n</i> -C20	282	$4.89 \times 10^{-8}$	$2.04 \times 10^{-8}$	$6.99 \times 10^{-8}$	$2.06 \times 10^{-8,c}$	90.3	99.4	108	102 <sup>c</sup>
heneicosane	<i>n</i> -C21	296	$1.42 \times 10^{-8}$	$7.76 \times 10^{-9}$	$2.42 \times 10^{-8}$	$(6.57-6.84) \times 10^{-9,c}$	95.0	104	113	107 <sup>c</sup>
docosane	<i>n</i> -C22	310	$6.86 \times 10^{-9}$	$3.09 \times 10^{-9}$	$8.40 \times 10^{-9}$	$(1.98-2.12) \times 10^{-9,c}$	97.8	110	117	112 <sup>c</sup>
tricosane	<i>n</i> -C23	324	$2.57 \times 10^{-9}$	$1.26 \times 10^{-9}$	$2.91 \times 10^{-9}$	$(2.07-7.14) \times 10^{-10,c}$	102	115	122	117 <sup>c</sup>
PAHs										
phenanthrene	PHE	178	$8.24 \times 10^{-8}$	$5.75 \times 10^{-7}$	$9.23 \times 10^{-7}$	$(7.34-9.90) \times 10^{-7,d}$	88.3	82.9	78.6	79.0-81.4 <sup>d</sup>
fluoranthene	FLU	202	$1.07 \times 10^{-9}$	$8.32 \times 10^{-8}$	$1.13 \times 10^{-7}$	$(4.73-11.9) \times 10^{-8,d}$	105	90.9	81.6	86.8-90.2 <sup>d</sup>
pyrene	PYR	202	$1.12 \times 10^{-10}$	$1.45 \times 10^{-7}$	$3.16 \times 10^{-8}$	$(3.76-8.62) \times 10^{-8,d}$	114	88.7	86.9	87.2-91.0 <sup>d</sup>
benz[a]anthracene	BaA	228	$2.49 \times 10^{-11}$	$3.98 \times 10^{-10}$	$3.40 \times 10^{-9}$	$(1.83-3.76) \times 10^{-9,d}$	119	107	108	95.3-104 <sup>d</sup>
chrysene/triphenylene	CT	228	$1.79 \times 10^{-11}$	$1.70 \times 10^{-10}$	$3.40 \times 10^{-9}$	$(1.68-1.76) \times 10^{-9,d}$	121	100	108	97.0-103 <sup>d</sup>

<sup>a</sup>Gou et al. (2021). <sup>b</sup>Xie et al. (2013, 2014). <sup>c</sup>Chickos and Hanshaw (2004) and references therein. <sup>d</sup>Haftka et al. (2006) and references therein.

values of other parameters in Equation 4 were set in accordance with previous studies ( $MW_{OM} = 200 \text{ g mol}^{-1}$  and  $\zeta_{OM} = 1.0$ ; Barsanti & Pankow, 2004; Williams et al., 2010; Xie et al., 2013, 2014). Due to the narrow range of literature  $p^{o,*}_L$  and  $Q^*_v$  (Table 1), their midranges were used for the prediction of  $K_{p,OM}$  for comparison.

To understand whether the inclusion of the adsorption mechanism can improve the simulation of the gas-particle partitioning, measured and predicted  $K_p$  values ( $K^m_{p,PM2.5}$  and  $K^t_{p,PM2.5}$ ) were calculated for comparison using Equations 1 and 2, where the mass concentration of TSP was replaced by that of  $PM_{2.5}$ . As shown in Table S1 in Supporting Information S1,  $N_s$  varied within an order of magnitude among different PM types ( $2.33 \times 10^{-10}$ – $9.47 \times 10^{-10} \text{ mol cm}^{-2}$ ). Although the  $a_{PM}$  value showed great variability across different PM sizes and types, the  $a_{PM}$  value of  $PM_{2.5}$  ( $a_{PM2.5}$ ) agreed well in different field studies ( $\sim 10 \text{ m}^2 \text{ g}^{-1}$ ). In Equation 2, the first term increases exponentially with the  $Q_l-Q_v$  value, which was initially used to fit measured  $K_p$  by assuming an equilibrium adsorption mechanism based on field data of organochlorines and PAHs and varied between 1 and 3 kcal mol<sup>-1</sup> (Bidleman et al., 1986; Bidleman & Foreman, 1987; Pankow, 1987; Yamasaki et al., 1982, 1984). When the absolute  $Q_l-Q_v$  value is close to 0, nearly liquid-like sorption is occurring. At  $T = 273 \text{ K}$ , the first term in the brackets of Equation 2 increases by more than two orders of magnitude, with the  $Q_l-Q_v$  value varying between 0 and 3 kcal mol<sup>-1</sup>. So, three  $Q_l-Q_v$  values (0, 1.5, and 3 kcal mol<sup>-1</sup>) were tested in this work for the comparison of  $K^m_{p,PM2.5}$  and  $K^t_{p,PM2.5}$ . For the calculation of  $K^t_{p,PM2.5}$ ,  $f_{OM}$  was the mass fraction of OM in  $PM_{2.5}$ ; an  $N_s$  value of  $4 \times 10^{14} \text{ cm}^2$  (or  $6.64 \times 10^{-10} \text{ mol cm}^2$ ), which lies between the values for TSP and soot particles, and an  $a_{PM2.5}$  value of  $10 \text{ m}^2 \text{ g}^{-1}$  were chosen.

### 3. Results and Discussion

#### 3.1. $\lg K^m_{p,OM}$ Versus $\lg K^t_{p,OM}$ Within Groups of Compounds

Table S2 summarizes the means and standard deviations of  $\lg K^m_{p,OM}$  and  $\lg K^t_{p,OM}$  for selected *n*-alkanes and PAHs, and Figure 1 compares the mean  $\lg K^m_{p,OM}$  and mean  $\lg K^t_{p,OM}$  by species. Generally, the  $p^{o,*}_L$  of *n*-alkanes predicted by the three methods and the corresponding  $K^t_{p,OM}$  values were of the same order of magnitude

**Table 2**  
Average Concentrations of *n*-Alkanes and PAHs in the Gas and Particle Phase and Their Particle-Phase Fractions (*F*%) in Nanjing and Denver

Species	Nanjing (2018–2019)			Denver (2012–2013)		
	Gas	Particle	<i>F</i> %	Gas	Particle	<i>F</i> %
<i>n</i> -Alkanes						
<i>n</i> -C18	15.4 ± 8.70	0.63 ± 0.75	5.64 ± 9.39 (96 <sup>a</sup> )	13.4 ± 11.5	0.92 ± 0.92	10.8 ± 15.4 (43)
<i>n</i> -C19	9.39 ± 5.43	0.79 ± 1.23	9.69 ± 15.7 (87)	6.94 ± 6.13	1.14 ± 1.25	21.6 ± 25.9 (49)
<i>n</i> -C20	6.86 ± 4.91	1.68 ± 1.85	23.9 ± 25.8 (100)	2.53 ± 2.36	0.82 ± 0.67	36.5 ± 29.6 (49)
<i>n</i> -C21	4.99 ± 3.91	2.48 ± 2.82	37.5 ± 36.2 (102)	1.31 ± 1.55	1.08 ± 0.62	58.8 ± 33.4 (50)
<i>n</i> -C22	3.74 ± 3.76	3.93 ± 4.69	50.4 ± 38.8 (90)	0.68 ± 0.86	1.06 ± 0.54	69.3 ± 29.1 (45)
<i>n</i> -C23	3.37 ± 4.32	5.26 ± 5.34	64.7 ± 33.6 (87)	0.66 ± 0.81	1.88 ± 1.47	79.1 ± 20.2 (38)
PAHs						
PHE	12.3 ± 8.42	0.44 ± 0.63	4.04 ± 6.71 (101)	9.51 ± 6.97	0.18 ± 0.22	4.13 ± 8.19 (45)
FLU	5.20 ± 3.97	1.11 ± 1.34	19.3 ± 18.9 (102)	1.07 ± 0.86	0.19 ± 0.21	21.7 ± 22.6 (49)
PYR	1.98 ± 1.92	0.88 ± 0.95	36.9 ± 29.1 (102)	0.31 ± 0.30	0.12 ± 0.17	37.7 ± 28.7 (46)
BaA	0.14 ± 0.15	0.80 ± 1.09	74.1 ± 22.6 (101)	0.026 ± 0.11	0.056 ± 0.087	71.3 ± 23.2 (25)
CT	0.29 ± 0.32	1.12 ± 1.25	71.9 ± 24.8 (102)	0.027 ± 0.050	0.15 ± 0.15	82.1 ± 18.0 (26)
Bulk components						
OC (μg m <sup>-3</sup> )	8.59 ± 3.68			3.17 ± 1.61		
PM <sub>2.5</sub> (μg m <sup>-3</sup> )	84.2 ± 37.4			9.51 ± 4.23		
rPM <sub>2.5</sub> (μg m <sup>-3</sup> ) <sup>b</sup>	46.6 ± 21.6					
Temp. (°C)	17.5 ± 9.26 (−5–36)			12.5 ± 10.1 (−13–29)		
RH (%)	67.9 ± 17.8% (24%–100%)			44.3 ± 17.8% (18%–90%)		

<sup>a</sup>Number of observations excluding missing values of the target compounds in the particle and/or gas phase.

<sup>b</sup>rPM<sub>2.5</sub> = NH<sub>4</sub><sup>+</sup> + Ca<sup>2+</sup> + Mg<sup>2+</sup> + K<sup>+</sup> + NO<sub>3</sub><sup>-</sup> + SO<sub>4</sub><sup>2-</sup> + OC × 1.6 + EC (Yang et al., 2021).

(Table 1, Table S2 in Supporting Information S1, and Figures 1a and 1c). When the SPARC method was applied to predict  $p^{o,*}_L$ , the scattering data of *n*-alkanes from Nanjing fell on the 1:1 line (Figure 1a), and those from Denver showed better agreement between  $\lg K^{m}_{p,OM}$  and  $\lg K^t_{p,OM}$ . As shown in Table 1 and Table S2 in Supporting Information S1, the SPARC  $p^{o,*}_L$  of the *n*-alkanes and the corresponding  $K^t_{p,OM}$  are in best agreement with the literature  $p^{o,*}_L$  and the derived  $K^t_{p,OM}$ . However, the mean  $K^{m}_{p,OM}$  values of the Denver *n*-alkanes were 2–20 times higher than the mean  $K^t_{p,OM}$ . These results suggest that the gas-particle partitioning of *n*-alkanes in Nanjing can be explained primarily by equilibrium absorption into the OM phase in PM, whereas in Denver other sorption mechanisms (e.g., adsorption) should contribute to the partitioning of *n*-alkanes into the particle phase.

The  $p^{o,*}_L$  values of the selected PAHs predicted by the TEST, SPARC, and SIMPOL methods varied by up to two orders of magnitude (Table 1). Only the scatter data based on SIMPOL estimation fell along a continuous line parallel to the identity line (Figures 1b and 1d). The comparisons of  $p^{o,*}_L$  values from this study and from the literature (Table 1) also indicate that the SIMPOL  $p^{o,*}_L$  of PAHs are the most reasonable estimates, and the mean  $\lg K^t_{p,OM}$  of PAHs based on SIMPOL  $p^{o,*}_L$  showed the best agreement with those based on literature  $p^{o,*}_L$  (Table S2 in Supporting Information S1). Although the regression line of  $\lg K^{m}_{p,OM}$  versus  $\lg K^t_{p,OM}$  has a slope close to 1.0 for both Nanjing (0.94) and Denver (1.15), the intercept (0.50 and 1.25) suggests stronger sorption to the PM phase than absorptive partitioning. Several studies tended to fit the  $\lg K^{m}_{p,OM}$  data of SVOCs in the same group by regression against their  $\lg p^o_L$  (Liang et al., 1997; Liang & Pankow, 1996; Mader & Pankow, 2002), but a significant correlation and a slope close to unity do not necessarily indicate the dominance of the equilibrium absorptive partitioning according to Equation 2. In our previous studies, the  $\lg K^{m}_{p,OM}$  of *n*-alkanes and PAHs were regressed on their  $\lg K^t_{p,OM}$  to evaluate the simulation of gas-particle partitioning (Gou et al., 2021; Xie et al., 2014), but the effects of  $p^{o,*}_L$  prediction were not considered, and the difference between  $K^{m}_{p,OM}$  and  $K^t_p$ .

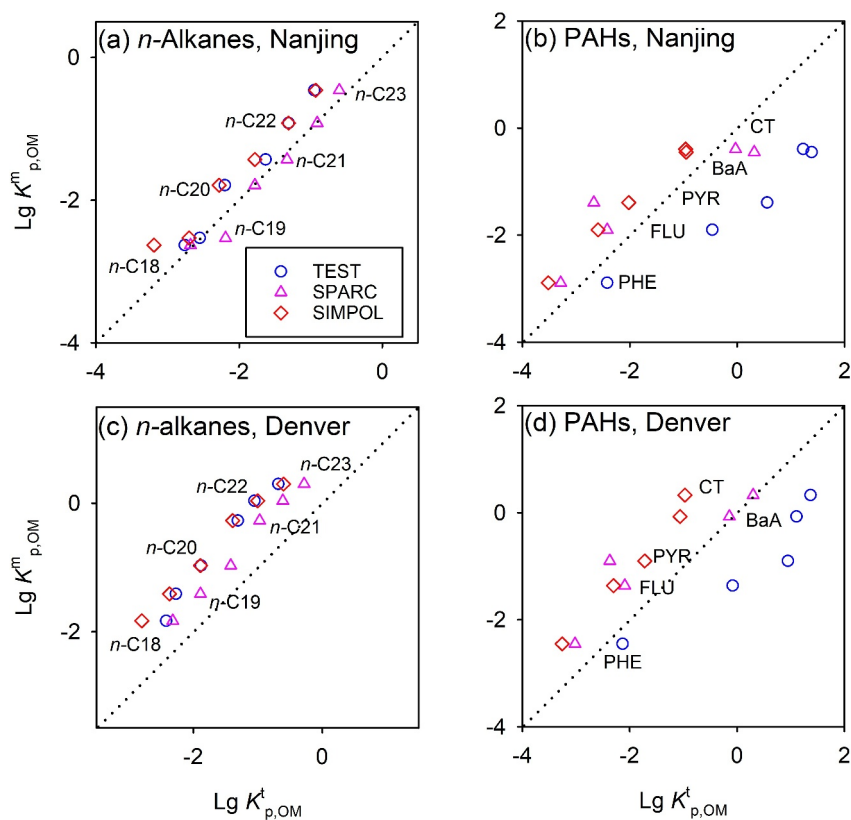


**Figure 1.** Comparisons of mean  $\lg K^m_{p,OM}$  and mean  $\lg K^t_{p,OM}$  for the selected *n*-alkanes and PAHs in panels (a, b) Nanjing and (c, d) Denver.

$K^m_{p,OM}$  can be up to two orders of magnitude. Even though the  $p^{0,*}_L$  prediction method was selected here in advance to improve the simulation of  $K^m_{p,OM}$ , noticeable differences between  $\lg K^m_{p,OM}$  and  $\lg K^t_{p,OM}$  were still observed.

### 3.2. $\lg K^m_{p,PM2.5}$ Versus $\lg K^t_{p,PM2.5}$ Within Groups of Compounds

When both the absorption and adsorption mechanisms were involved for the prediction of the partitioning coefficient, the  $p^{0,*}_L$  values of selected *n*-alkanes and PAHs were preferably estimated using the SPARC and SIMPOL methods, respectively, as they perform well in reproducing literature  $p^{0,*}_L$  values and predicting  $K_{p,OM}$ . The means and standard deviations of  $\lg K^m_{p,PM2.5}$  and  $\lg K^t_{p,PM2.5}$  based on Nanjing and Denver data are shown in Table S3 in Supporting Information S1. Using SPARC  $p^{0,*}_L$  and a  $Q_l-Q_v$  value of 0 kcal mol<sup>-1</sup>, the mean  $\lg K^m_{p,PM2.5}$  and  $\lg K^t_{p,PM2.5}$  of the selected *n*-alkanes in Nanjing were almost identical (Table S3 in Supporting Information S1 and Figure 2a). However, in Denver, the  $Q_l-Q_v$  value needs to be increased to a value between 1.5 and 3.0 kcal mol<sup>-1</sup> to achieve a good match (Figure 2c). When  $p^{0,*}_L$  was predicted by the TEST or SPARC method, the agreement between  $\lg K^m_{p,PM2.5}$  and  $\lg K^t_{p,PM2.5}$  cannot be obtained by assuming a single  $Q_l-Q_v$  value for all PAH species (Figures S1 and S2 in Supporting Information S1). In both Nanjing and Denver, the selected PAHs had greater  $Q_l-Q_v$  values than the *n*-alkanes (Figure 2). Table S4 in Supporting Information S1 provides the selection of  $Q_l-Q_v$  that best fit the mean  $\lg K^m_{p,PM2.5}$  for *n*-alkanes and PAHs in Nanjing (0 and 2 kcal mol<sup>-1</sup>) and Denver (2.6 and 3 kcal mol<sup>-1</sup>) by retrieving the minimum average relative percent difference (ARPD, %). Thus, if the  $p^{0,*}_L$  and  $Q_l-Q_v$  values are estimated appropriately, the inclusion of the adsorption mechanism can improve the simulation of gas-particle partitioning for the selected *n*-alkanes and PAHs.

A very small  $Q_l-Q_v$  value in the order of 0.25 kcal mol<sup>-1</sup> usually indicates liquid-like sorption (Pankow, 1987), and there is evidence that the complex mixtures of solid-like organic compounds in aerosols behave like a liquid (Cappa et al., 2008). However, the results shown here suggest that sorption is not liquid-like, especially for the

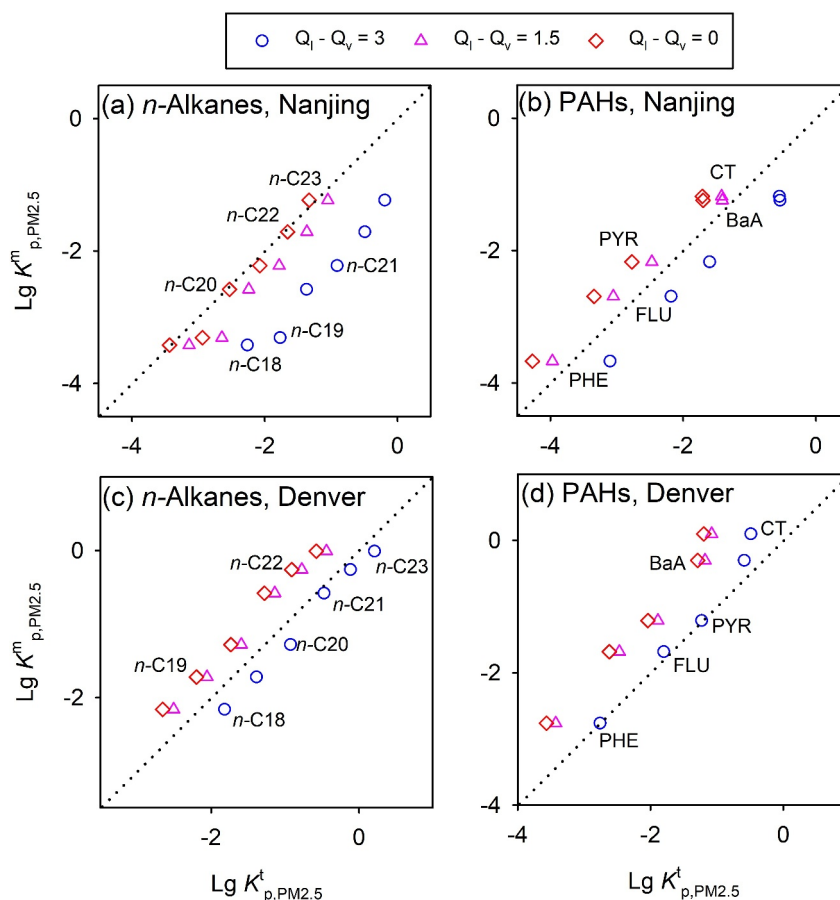


**Figure 2.** Comparisons of mean  $\lg K^m_{p,PM2.5}$  and mean  $\lg K^t_{p,PM2.5}$  for the selected *n*-alkanes and PAHs in panels (a, b) Nanjing and (c, d) Denver. The  $p^{0*}_L$  values of the selected *n*-alkanes and PAHs were predicted using the SPARC and SIMPOL methods, respectively.

target SVOCs in Denver. Compared to Nanjing, Denver has a much lower average humidity (Table 2), and ambient aerosols were expected to have low ALW content (Carlton & Turpin, 2013). Moreover, ambient air in Denver may contain more non-exchangeable *n*-alkanes and PAHs trapped in the PM or bound to highly active sites (Bidleman et al., 1986; Harner & Bidleman, 1998), resulting in a very slow equilibrium between the gas and particle phases. Despite the aerosol phase state is not completely clear, comparisons between Figures 1 and 2 show that physical adsorption plays an important role in the gas-particle partitioning. Based on the optimal selection of the  $p^{0*}_L$  estimation method and the  $Q_l - Q_v$  values in Table S4 in Supporting Information S1, the adsorption mechanism contributes to 7.75% of the  $K^t_{p,PM2.5}$  for the selected *n*-alkanes in Nanjing, supporting that the absorption mechanism dominates the gas-particle partitioning of *n*-alkanes in Nanjing. However, more than 70% of the  $K^t_{p,PM2.5}$  for the selected PAHs in Nanjing and the target SVOCs in Denver were caused by the adsorption mechanism.

The dry mass of  $PM_{2.5}$  is well reconstructed by inorganic ions, OC, and EC in Nanjing (Xie et al., 2022; Yu et al., 2020). In most air quality monitoring stations, hourly  $PM_{2.5}$  concentrations were recorded at a relative humidity of <35% to minimize ALW content and avoid over-measuring. To understand whether dry  $PM_{2.5}$  mass data can be used to parameterize the gas-particle partitioning of SVOCs in Nanjing, we proposed a partitioning between gas phase and reconstructed  $PM_{2.5}$  ( $rPM_{2.5}$ ) in Text S1 in Supporting Information S1. The concentration of  $rPM_{2.5}$  was calculated as the sum of the measured inorganic ions, OM ( $OC \times 1.6$ ), and EC (Table 2), and the mass fraction of OM in  $rPM_{2.5}$  was used instead of  $f_{OM}$  to calculate  $K^t_{p,rPM2.5}$ . Table S5 in Supporting Information S1 lists the means and standard deviations of  $\lg K^m_{p,rPM2.5}$  and  $\lg K^t_{p,rPM2.5}$  based on the Nanjing data. Similar to the simulation of  $K^m_{p,PM2.5}$ , the agreement between  $\lg K^m_{p,PM2.5}$  and  $\lg K^t_{p,rPM2.5}$  was satisfactory for all species when their  $p^{0*}_L$  estimation method and  $Q_l - Q_v$  values were appropriately chosen (Figure S3 and Table

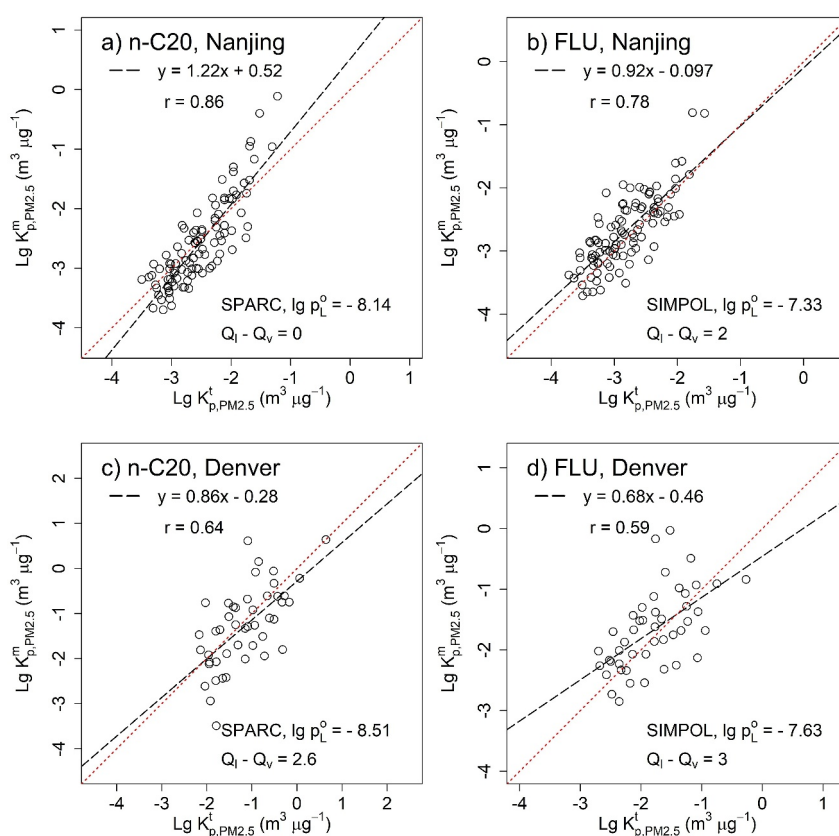


**Figure 3.** Comparisons of  $\lg K^m_{p,PM2.5}$  and  $\lg K^t_{p,PM2.5}$  for *n*-C20 and FLU in panels (a, b) Nanjing and (c, d) Denver. The selection of  $p^{0,*}_L$  estimation method and  $Q_l - Q_v$  values are shown in Table S4 in Supporting Information S1.

S4 in Supporting Information S1). Compared to sorption to  $PM_{2.5}$ , sorption of the selected PAHs to  $rPM_{2.5}$  appears less liquid-like ( $Q_l - Q_v = 2.4 \text{ kcal mol}^{-1}$ ; Table S4 in Supporting Information S1) possibly due to the exclusion of ALW.

### 3.3. $\lg K^m_{p,PM2.5}$ Versus $\lg K^t_{p,PM2.5}$ for Individual Compounds

Owing to the variations in ambient temperature (Table 2), the partitioning coefficient of the individual species can vary by several orders of magnitude within a year. To assess the simulation of temporal variations in partitioning coefficients, the  $\lg K^m_{p,PM2.5}$  and  $\lg K^t_{p,PM2.5}$  of *n*-C20 and FLU in Nanjing and Denver are compared for all samples in Figure 3, and the comparisons for other species are shown in Figures S4 and S5 in Supporting Information S1. For the calculation of  $K^t_{p,PM2.5}$ , the selection of  $p^{0,*}_L$  estimation methods and  $Q_l - Q_v$  values given in Table S4 in Supporting Information S1 were used. The scattering data of most species in Nanjing followed a continuous line, and all regression slopes of PAHs are close to 1.0 (0.92–1.05). However, for *n*-alkanes with carbon number >20, the regression slopes were well above 1.0 (Figures S4c–S4e in Supporting Information S1), which was attributed to deviations from true equilibrium sorption, measurement artifacts, or changes in sorbent properties (Goss & Schwarzenbach, 1998; Pankow & Bidleman, 1992).

In this work, the gas-particle partitioning of selected *n*-alkanes and PAHs was predicted based on established absorptive and adsorptive mechanisms without considering the phase state of the particles, which can change with aerosol composition and meteorological conditions (e.g., temperature and humidity; Shiraiwa et al., 2017; Liu et al., 2019). Once the aerosol phase state changes from a liquid to a semisolid or glassy state, the partitioning of SVOCs can be kinetically inhibited, resulting in longer equilibration time scales or even non-equilibrium partitioning (Koop et al., 2011; Shiraiwa et al., 2013; Virtanen et al., 2010; Zobrist et al., 2008). Given the dependence of aerosol phase state on temperature (Petters et al., 2019; Slade et al., 2017) and the limited number



of sample pairs in this work, the comparisons of  $\lg K_{p,PM2.5}^m$  and  $\lg K_{p,PM2.5}^l$  of *n*-C20 and FLU are divided into two groups by temperature in Figure S6 in Supporting Information S1. It can be seen that the regression slopes show a larger deviation from unity in lower temperature ranges, which may be partly ascribed to the change of aerosol phase state with temperature. In addition, integrated sampling was conducted in Nanjing and Denver for 12 and 24 hr, respectively, when the ambient temperature and atmospheric concentrations fluctuated. In this case, the target compounds could condense or evaporate on the particles originally collected on the filter during each sampling interval. Therefore, the *F* and *A* values of each pair of samples can hardly reflect the averaged instantaneous concentrations of SVOCs in the particulate and gas phases. Gou et al. (2021) found that the regression slopes of  $\lg K_{p,OM}^m$  and  $\lg K_{p,OM}^l$  depend on how the sampling artifact was adjusted based on  $Q_b$  measurements. Here, we roughly divided the  $Q_b$  concentrations equally into positive and negative artifacts, which could also be a possible reason for the deviation of the regression slopes from 1.0. But unfortunately, it is not possible to obtain unbiased *F* and *A* values with the current sampling method. For future studies, highly time-resolved measurements are required to reduce the effects of variations in temperature and atmospheric concentrations during sampling, and the effects of changes in the phase state of atmospheric aerosols on the partitioning of SVOCs need to be quantitatively evaluated.

As shown in Figures 3c and 3d and Figure S5 in Supporting Information S1, the comparisons of  $\lg K_{p,PM2.5}^m$  and  $\lg K_{p,PM2.5}^l$  for the target compounds are more scattered in Denver than in Nanjing, although the data for most species are almost evenly distributed on the two sides of the identity line. Because Denver has a longer cold period and lower temperatures than Nanjing, and the average concentrations of the low-volatility *n*-alkanes and PAHs were also much lower in Denver than in Nanjing (Table 2), the gas-phase concentrations of the heavier *n*-alkanes and PAHs in Denver were subject to greater uncertainties. Mader and Pankow (2002) found that normalization of  $K_p$  values by  $f_{OM}$  can reduce the degree of variation in the partitioning data ( $\lg K_{p,OM}^m$  vs.  $\lg p_L^o$ ). This phenomenon was also observed in Denver in the comparisons of  $\lg K_{p,OM}^m$  and  $\lg K_{p,OM}^l$  (Figure S7 in Supporting Information S1), but not in Nanjing (Figure S8 in Supporting Information S1). It is therefore suspected that the adsorption-dominated  $K_{p,PM2.5}^m$  in Denver is more influenced by the change in aerosol phase state and biased *F* and *A* during integrated sampling than in Nanjing.

#### 4. Conclusions

The comparison results of  $\lg K_{p,OM}^m$  and  $\lg K_{p,OM}^l$  show that the gas-particle partitioning of semi-volatile *n*-alkanes in Nanjing can be predicted quite well by the equilibrium absorptive partitioning theory, which, however, cannot fully explain the sorption of *n*-alkanes in Denver. Even if the estimation method of  $p_L^{o,*}$  was preselected to improve the agreement between  $\lg K_{p,OM}^m$  and  $\lg K_{p,OM}^l$ , PAHs exhibited stronger sorption to  $PM_{2.5}$  than the prediction based on OM absorption. Good agreement between  $\lg K_{p,PM2.5}^m$  and  $\lg K_{p,PM2.5}^l$  can be obtained by selecting the  $p_L^{o,*}$  estimation method and the  $Q_l-Q_v$  value for both the Nanjing and Denver data. Unlike *n*-alkanes in Nanjing, the adsorption mechanism in Denver dominates the gas-particle partitioning of all selected SVOCs, and the sorption is less liquid-like, which may be due to the low ALW content. Besides the mean values of  $\lg K_{p,PM2.5}^m$  within groups of compounds, temporal variations were also adequately reflected by  $\lg K_{p,PM2.5}^l$ . Thus, the prediction of the gas-particle partitioning behavior of non-polar SVOCs considering absorption and adsorption mechanisms is promising. Since the variations in aerosol phase state, ambient temperature, and atmospheric concentrations during integrated sampling are responsible for the difference between measured and predicted partitioning coefficients, more efforts (e.g., highly time-resolved measurements) are needed to address these issues in future studies.

#### Conflict of Interest

The authors declare no conflicts of interest relevant to this study.

#### Data Availability Statement

Data used in the writing of this paper (and its Supporting Information S1 file) are publicly available on Harvard Dataverse (Zhou et al., 2023; <https://doi.org/10.7910/DVN/QH7EYO>).

**Acknowledgments**

This work was supported by the National Natural Science Foundation of China (NSFC, 42007325, 42177211).

**References**

Barsanti, K. C., Carlton, A. G., & Chung, S. H. (2013). Analyzing experimental data and model parameters: Implications for predictions of SOA using chemical transport models. *Atmospheric Chemistry and Physics*, 13(23), 12073–12088. <https://doi.org/10.5194/acp-13-12073-2013>

Barsanti, K. C., & Pankow, J. F. (2004). Thermodynamics of the formation of atmospheric organic particulate matter by accretion reactions—Part 1: Aldehydes and ketones. *Atmospheric Environment*, 38(26), 4371–4382. <https://doi.org/10.1016/j.atmosenv.2004.03.035>

Beardsley, R. L., & Jang, M. (2016). Simulating the SOA formation of isoprene from partitioning and aerosol phase reactions in the presence of inorganics. *Atmospheric Chemistry and Physics*, 16(9), 5993–6009. <https://doi.org/10.5194/acp-16-5993-2016>

Bidleman, T. F. (1988). Atmospheric processes. *Environmental Science & Technology*, 22(4), 361–367. <https://doi.org/10.1021/es00169a002>

Bidleman, T. F., Billings, W. N., & Foreman, W. T. (1986). Vapor-particle partitioning of semivolatile organic compounds: Estimates from field collections. *Environmental Science & Technology*, 20(10), 1038–1043. <https://doi.org/10.1021/es00152a013>

Bidleman, T. F., & Foreman, W. T. (1987). Vapor-particle partitioning of semivolatile organic compounds. In *Sources and fates of aquatic pollutants* (Vol. 216, pp. 27–56). American Chemical Society. <https://doi.org/10.1021/ba-1987-0216.ch002>

Cappa, C. D., Lovejoy, E. R., & Ravishankara, A. R. (2008). Evidence for liquid-like and nonideal behavior of a mixture of organic aerosol components. *Proceedings of the National Academy of Sciences*, 105(48), 18687–18691. <https://doi.org/10.1073/pnas.0802144105>

Carlton, A. G., & Turpin, B. J. (2013). Particle partitioning potential of organic compounds is highest in the Eastern US and driven by anthropogenic water. *Atmospheric Chemistry and Physics*, 13(20), 10203–10214. <https://doi.org/10.5194/acp-13-10203-2013>

Chang, E. I., & Pankow, J. F. (2010). Organic particulate matter formation at varying relative humidity using surrogate secondary and primary organic compounds with activity corrections in the condensed phase obtained using a method based on the Wilson equation. *Atmospheric Chemistry and Physics*, 10(12), 5475–5490. <https://doi.org/10.5194/acp-10-5475-2010>

Chickos, J. S., & Hanshaw, W. (2004). Vapor pressures and vaporization enthalpies of the n-alkanes from C21 to C30 at T = 298.15 K by correlation gas chromatography. *Journal of Chemical & Engineering Data*, 49(1), 77–85. <https://doi.org/10.1021/jc0301747>

Cousins, I. T., & Mackay, D. (2001). Gas-particle partitioning of organic compounds and its interpretation using relative solubilities. *Environmental Science & Technology*, 35(4), 643–647. <https://doi.org/10.1021/es001123m>

Daumit, K. E., Carrasquillo, A. J., Sugrue, R. A., & Kroll, J. H. (2016). Effects of condensed-phase oxidants on secondary organic aerosol formation. *The Journal of Physical Chemistry A*, 120(9), 1386–1394. <https://doi.org/10.1021/acs.jpca.5b06160>

Donahue, N. M., Robinson, A. L., Stanier, C. O., & Pandis, S. N. (2006). Coupled partitioning, dilution, and chemical aging of semivolatile organics. *Environmental Science & Technology*, 40(8), 2635–2643. <https://doi.org/10.1021/es052297c>

EPA. (2022). Toxicity Estimation Software Tool (TEST). The United States Environmental Protection Agency’s Center for Computational Toxicology and Exposure. <https://doi.org/10.23645/epacomptox.21379365.v3>

Goss, K.-U., & Schwarzenbach, R. P. (1998). Gas/solid and gas/liquid partitioning of organic compounds: Critical evaluation of the interpretation of equilibrium constants. *Environmental Science & Technology*, 32(14), 2025–2032. <https://doi.org/10.1021/es9710518>

Gou, Y., Qin, C., Liao, H., & Xie, M. (2021). Measurements, gas/particle partitioning, and sources of nonpolar organic molecular markers at a suburban site in the west Yangtze River Delta, China. *Journal of Geophysical Research: Atmospheres*, 126(19), e2020JD034080. <https://doi.org/10.1029/2020JD034080>

Haftka, J. J. H., Parsons, J. R., & Govers, H. A. J. (2006). Supercooled liquid vapour pressures and related thermodynamic properties of polycyclic aromatic hydrocarbons determined by gas chromatography. *Journal of Chromatography A*, 1135(1), 91–100. <https://doi.org/10.1016/j.chroma.2006.09.050>

Hallquist, M., Wenger, J. C., Baltensperger, U., Rudich, Y., Simpson, D., Claeys, M., et al. (2009). The formation, properties and impact of secondary organic aerosol: Current and emerging issues. *Atmospheric Chemistry and Physics*, 9(14), 5155–5236. <https://doi.org/10.5194/acp-9-5155-2009>

Harner, T., & Bidleman, T. F. (1998). Octanol–air partition coefficient for describing particle/gas partitioning of aromatic compounds in urban air. *Environmental Science & Technology*, 32(10), 1494–1502. <https://doi.org/10.1021/es970890r>

Healy, R. M., Wenger, J. C., Metzger, A., Duplissy, J., Kalberer, M., & Dommen, J. (2008). Gas/particle partitioning of carbonyls in the photooxidation of isoprene and 1,3,5-trimethylbenzene. *Atmospheric Chemistry and Physics*, 8(12), 3215–3230. <https://doi.org/10.5194/acp-8-3215-2008>

Kampf, C. J., Waxman, E. M., Slowik, J. G., Dommen, J., Pfaffenberger, L., Praplan, A. P., et al. (2013). Effective Henry’s law partitioning and the salting constant of glyoxal in aerosols containing sulfate. *Environmental Science & Technology*, 47(9), 4236–4244. <https://doi.org/10.1021/es400083d>

Koop, T., Bookhold, J., Shiraiwa, M., & Pöschl, U. (2011). Glass transition and phase state of organic compounds: Dependency on molecular properties and implications for secondary organic aerosols in the atmosphere. *Physical Chemistry Chemical Physics*, 13(43), 19238–19255. <https://doi.org/10.1039/C1CP22617G>

Liang, C., & Pankow, J. F. (1996). Gas/particle partitioning of organic compounds to environmental tobacco smoke: Partition coefficient measurements by desorption and comparison to urban particulate material. *Environmental Science & Technology*, 30(9), 2800–2805. <https://doi.org/10.1021/es960050x>

Liang, C., Pankow, J. F., Odum, J. R., & Seinfeld, J. H. (1997). Gas/particle partitioning of semivolatile organic compounds to model inorganic, organic, and ambient smog aerosols. *Environmental Science & Technology*, 31(11), 3086–3092. <https://doi.org/10.1021/es9702529>

Liu, Y., Wu, Z., Huang, X., Shen, H., Bai, Y., Qiao, K., et al. (2019). Aerosol phase state and its link to chemical composition and liquid water content in a subtropical coastal megacity. *Environmental Science & Technology*, 53(9), 5027–5033. <https://doi.org/10.1021/acs.est.9b01196>

Mader, B. T., & Pankow, J. F. (2002). Study of the effects of particle-phase carbon on the gas/particle partitioning of semivolatile organic compounds in the atmosphere using controlled field experiments. *Environmental Science & Technology*, 36(23), 5218–5228. <https://doi.org/10.1021/es011048v>

Odum, J. R., Hoffmann, T., Bowman, F., Collins, D., Flagan, R. C., & Seinfeld, J. H. (1996). Gas/particle partitioning and secondary organic aerosol yields. *Environmental Science & Technology*, 30(8), 2580–2585. <https://doi.org/10.1021/es950943+>

Pankow, J. F. (1987). Review and comparative analysis of the theories on partitioning between the gas and aerosol particulate phases in the atmosphere. *Atmospheric Environment*, 21(11), 2275–2283. [https://doi.org/10.1016/0004-6981\(87\)90363-5](https://doi.org/10.1016/0004-6981(87)90363-5)

Pankow, J. F. (1994a). An absorption model of gas/particle partitioning of organic compounds in the atmosphere. *Atmospheric Environment*, 28(2), 185–188. [https://doi.org/10.1016/1352-2310\(94\)90093-0](https://doi.org/10.1016/1352-2310(94)90093-0)

Pankow, J. F. (1994b). An absorption model of the gas/aerosol partitioning involved in the formation of secondary organic aerosol. *Atmospheric Environment*, 28(2), 189–193. [https://doi.org/10.1016/1352-2310\(94\)90094-9](https://doi.org/10.1016/1352-2310(94)90094-9)

- Pankow, J. F., & Asher, W. E. (2008). SIMPOL.1: A simple group contribution method for predicting vapor pressures and enthalpies of vaporization of multifunctional organic compounds. *Atmospheric Chemistry and Physics*, 8(10), 2773–2796. <https://doi.org/10.5194/acp-8-2773-2008>
- Pankow, J. F., & Bidleman, T. F. (1992). Interdependence of the slopes and intercepts from log-log correlations of measured gas-particle partitioning and vapor pressure—I. Theory and analysis of available data. *Atmospheric Environment, Part A: General Topics*, 26(6), 1071–1080. [https://doi.org/10.1016/0960-1686\(92\)90039-N](https://doi.org/10.1016/0960-1686(92)90039-N)
- Pankow, J. F., & Chang, E. I. (2008). Variation in the sensitivity of predicted levels of atmospheric organic particulate matter (OPM). *Environmental Science & Technology*, 42(19), 7321–7329. <https://doi.org/10.1021/es8003377>
- Petters, S. S., Kreidenweis, S. M., Grieshop, A. P., Ziemann, P. J., & Petters, M. D. (2019). Temperature- and humidity-dependent phase states of secondary organic aerosols. *Geophysical Research Letters*, 46(2), 1005–1013. <https://doi.org/10.1029/2018GL080563>
- Pye, H. O. T., Murphy, B. N., Xu, L., Ng, N. L., Carlton, A. G., Guo, H., et al. (2017). On the implications of aerosol liquid water and phase separation for organic aerosol mass. *Atmospheric Chemistry and Physics*, 17(1), 343–369. <https://doi.org/10.5194/acp-17-343-2017>
- Shiraiwa, M., Li, Y., Tsimpidi, A. P., Karydis, V. A., Berkemeier, T., Pandis, S. N., et al. (2017). Global distribution of particle phase state in atmospheric secondary organic aerosols. *Nature Communications*, 8(1), 15002. <https://doi.org/10.1038/ncomms15002>
- Shiraiwa, M., Zuend, A., Bertram, A. K., & Seinfeld, J. H. (2013). Gas-particle partitioning of atmospheric aerosols: Interplay of physical state, non-ideal mixing and morphology. *Physical Chemistry Chemical Physics*, 15(27), 11441–11453. <https://doi.org/10.1039/C3CP51595H>
- Slade, J. H., Shiraiwa, M., Arangio, A., Su, H., Pöschl, U., Wang, J., & Knopf, D. A. (2017). Cloud droplet activation through oxidation of organic aerosol influenced by temperature and particle phase state. *Geophysical Research Letters*, 44(3), 1583–1591. <https://doi.org/10.1002/2016GL072424>
- Turpin, B. J., & Lim, H.-J. (2001). Species contributions to PM<sub>2.5</sub> mass concentrations: Revisiting common assumptions for estimating organic mass. *Aerosol Science and Technology*, 35(1), 602–610. <https://doi.org/10.1080/02786820119445>
- Virtanen, A., Joutsensaari, J., Koop, T., Kannosto, J., Yli-Pirilä, P., Leskinen, J., et al. (2010). An amorphous solid state of biogenic secondary organic aerosol particles. *Nature*, 467(7317), 824–827. <https://doi.org/10.1038/nature09455>
- Wang, X., Bi, C., & Xu, Y. (2015). Modeling and analysis of sampling artifacts in measurements of gas-particle partitioning of semivolatile organic contaminants using filter-sorbent samplers. *Atmospheric Environment*, 117, 99–109. <https://doi.org/10.1016/j.atmosenv.2015.06.053>
- Weschler, C. J., & Nazaroff, W. W. (2008). Semivolatile organic compounds in indoor environments. *Atmospheric Environment*, 42(40), 9018–9040. <https://doi.org/10.1016/j.atmosenv.2008.09.052>
- Williams, B. J., Goldstein, A. H., Kreisberg, N. M., & Hering, S. V. (2010). In situ measurements of gas/particle-phase transitions for atmospheric semivolatile organic compounds. *Proceedings of the National Academy of Sciences*, 107(15), 6676–6681. <https://doi.org/10.1073/pnas.0911858107>
- Xie, M., Barsanti, K. C., Hannigan, M. P., Dutton, S. J., & Vedal, S. (2013). Positive matrix factorization of PM<sub>2.5</sub> - Eliminating the effects of gas/particle partitioning of semivolatile organic compounds. *Atmospheric Chemistry and Physics*, 13(15), 7381–7393. <https://doi.org/10.5194/acp-13-7381-2013>
- Xie, M., Hannigan, M. P., & Barsanti, K. C. (2014). Gas/particle partitioning of n-alkanes, PAHs and oxygenated PAHs in urban Denver. *Atmospheric Environment*, 95(0), 355–362. <https://doi.org/10.1016/j.atmosenv.2014.06.056>
- Xie, M., Lu, X., Ding, F., Cui, W., Zhang, Y., & Feng, W. (2022). Evaluating the influence of constant source profile presumption on PMF analysis of PM<sub>2.5</sub> by comparing long- and short-term hourly observation-based modeling. *Environmental Pollution*, 314, 120273. <https://doi.org/10.1016/j.envpol.2022.120273>
- Yamasaki, H., Kuwata, K., & Kuge, Y. (1984). Determination of vapor pressure of polycyclic aromatic hydrocarbons in the supercooled liquid phase and their adsorption on airborne particulate matter. *Nippon Kagaku Kaishi*, 1984(8), 1324–1329. <https://doi.org/10.1246/nikkashi.1984.1324>
- Yamasaki, H., Kuwata, K., & Miyamoto, H. (1982). Effects of ambient temperature on aspects of airborne polycyclic aromatic hydrocarbons. *Environmental Science & Technology*, 16(4), 189–194. <https://doi.org/10.1021/es00098a003>
- Yang, L., Shang, Y., Hannigan, M. P., Zhu, R., Wang, Q. g., Qin, C., & Xie, M. (2021). Collocated speciation of PM<sub>2.5</sub> using tandem quartz filters in northern Nanjing, China: Sampling artifacts and measurement uncertainty. *Atmospheric Environment*, 246, 118066. <https://doi.org/10.1016/j.atmosenv.2020.118066>
- Yu, Y., Ding, F., Mu, Y., Xie, M., & Wang, Q. g. (2020). High time-resolved PM<sub>2.5</sub> composition and sources at an urban site in Yangtze River Delta, China after the implementation of the APPCAP. *Chemosphere*, 261, 127746. <https://doi.org/10.1016/j.chemosphere.2020.127746>
- Yu, Z., Jang, M., Zhang, T., Madhu, A., & Han, S. (2021). Simulation of monoterpene SOA formation by multiphase reactions using explicit mechanisms. *ACS Earth and Space Chemistry*, 5(6), 1455–1467. <https://doi.org/10.1021/acsearthspacechem.1c00056>
- Zhang, J., He, X., Ding, X., Yu, J. Z., & Ying, Q. (2022). Modeling secondary organic aerosol tracers and tracer-to-SOA ratios for monoterpenes and sesquiterpenes using a chemical transport model. *Environmental Science & Technology*, 56(2), 804–813. <https://doi.org/10.1021/acs.est.1c06373>
- Zhou, Z., Wang, Z., Feng, W., Qin, C., Liao, H., Wang, Y., & Xie, M. (2023). Replication data for: Simulation of gas-particle partitioning of semivolatile n-alkanes and PAHs in Nanjing and Denver (version 2) [Dataset]. *Harvard Dataverse*. <https://doi.org/10.7910/DVN/QH7EYO>
- Zhu, D., Hyun, S., Pignatello, J. J., & Lee, L. S. (2004). Evidence for  $\pi$ - $\pi$  electron donor-acceptor interactions between  $\pi$ -donor aromatic compounds and  $\pi$ -acceptor sites in soil organic matter through pH effects on sorption. *Environmental Science & Technology*, 38(16), 4361–4368. <https://doi.org/10.1021/es035379e>
- Zobrist, B., Marcolli, C., Pedernera, D. A., & Koop, T. (2008). Do atmospheric aerosols form glasses? *Atmospheric Chemistry and Physics*, 8(17), 5221–5244. <https://doi.org/10.5194/acp-8-5221-2008>

## References From the Supporting Information

- Cachon, F. B., Cazier, F., Verdin, A., Dewaele, D., Genevray, P., Delbende, A., et al. (2023). Physicochemical characterization of air pollution particulate matter (PM<sub>2.5</sub> and PM<sub>2.5-10</sub>) in an urban area of Cotonou, Benin. *Atmosphere*, 14(2), 201. <https://doi.org/10.3390/atmos14020201>
- Courcot, D., Laversin, H., Ledoux, F., Cazier, F., Matta, J., Cousin, R., & Aboukais, A. (2009). Composition and textural properties of soot and study of their oxidative elimination by catalytic process. *International Journal of Environment and Pollution*, 39(3–4), 253–263. <https://doi.org/10.1504/IJEP.2009.028689>
- Gustafsson, Ö., Bucheli, T. D., Kukulska, Z., Andersson, M., Largeau, C., Rouzaud, J.-N., et al. (2001). Evaluation of a protocol for the quantification of black carbon in sediments. *Global Biogeochemical Cycles*, 15(4), 881–890. <https://doi.org/10.1029/2000GB001380>

- Hanisch, F., & Crowley, J. N. (2003). Ozone decomposition on Saharan dust: An experimental investigation. *Atmospheric Chemistry and Physics*, 3(1), 119–130. <https://doi.org/10.5194/acp-3-119-2003>
- Kouassi, K. S., Billet, S., Garçon, G., Verdin, A., Diouf, A., Cazier, F., et al. (2010). Oxidative damage induced in A549 cells by physically and chemically characterized air particulate matter (PM<sub>2.5</sub>) collected in Abidjan, Côte d'Ivoire. *Journal of Applied Toxicology*, 30(4), 310–320. <https://doi.org/10.1002/jat.1496>
- Ndong Ba, A., Cazier, F., Verdin, A., Garçon, G., Cabral, M., Courcot, L., et al. (2019). Physico-chemical characterization and in vitro inflammatory and oxidative potency of atmospheric particles collected in Dakar city's (Senegal). *Environmental Pollution*, 245, 568–581. <https://doi.org/10.1016/j.envpol.2018.11.026>
- Popovitcheva, O. B., Persiantseva, N. M., Trukhin, M. E., Rulev, G. B., Shonija, N. K., Buriko, Y. Y., et al. (2000). Experimental characterization of aircraft combustor soot: Microstructure, surface area, porosity and water adsorption. *Physical Chemistry Chemical Physics*, 2(19), 4421–4426. <https://doi.org/10.1039/B004345L>
- Pöschl, U., Letzel, T., Schauer, C., & Niessner, R. (2001). Interaction of ozone and water vapor with spark discharge soot aerosol particles coated with benzo[a]pyrene: O<sub>3</sub> and H<sub>2</sub>O adsorption, benzo[a]pyrene degradation, and atmospheric implications. *The Journal of Physical Chemistry A*, 105(16), 4029–4041. <https://doi.org/10.1021/jp004137n>
- Roth, C. M., Goss, K.-U., & Schwarzenbach, R. P. (2005). Sorption of a diverse Set of organic vapors to diesel soot and road tunnel aerosols. *Environmental Science & Technology*, 39(17), 6632–6637. <https://doi.org/10.1021/es049204w>
- Sullivan, R. C., Thornberry, T., & Abbatt, J. P. D. (2004). Ozone decomposition kinetics on alumina: Effects of ozone partial pressure, relative humidity and repeated oxidation cycles. *Atmospheric Chemistry and Physics*, 4(5), 1301–1310. <https://doi.org/10.5194/acp-4-1301-2004>